JOURNAL OF APPLIED ELECTROCHEMISTRY 24 (1994) 1124–1132

Calculation of bypass currents in molten salt bipolar cells

I. ROUSAR*, J. THONSTAD

Department of Electrochemistry, Norwegian Institute of Technology, N-7034 Trondheim, Norway

Received 27 August 1993; revised 18 April 1994

A theoretical model is given for calculation of parasitic currents (bypass currents) for a stack of bipolar cells used in molten salt electrolysis. A simplified bypass current calculation was confirmed by the numerical solution of the Laplace equation for Galvani potentials in the interelectrode space and in the free space of the cell stack for the aluminium cell of the 'Alcoa Smelting Process' ($AlCl_3$ electrolysis) with 11 bipolar electrodes. Due to the bypass currents the current efficiency of the electrochemical process was lowered to 82%–94%, depending on the height of the stack, i.e. the thickness of the bipolar electrodes. These values were in a good agreement with values obtained on the basis of the simplified approach. The numerical solution of the Laplace equation allowed a detailed description of the influence of the bypass current flow on the current distribution at the edges of the bipolar electrodes.

List of symbols

a	dimensionless parameter, see Equation 12
A_E	floor area of horizontally placed bipolar electrodes (cm^2)
A_F	cross-sectional area of the downcomers and the upcomer (cm^2)
b	dimensionless parameter, see Equation 13
d_E	thickness of the bipolar electrode (cm)
d_G	the interelectrode gap (cm)
E	electrode potential (V)
E_r	reversible electrode potential (V)
f_E	average fraction of current used for metal production in the bipolar stack, see Equations 9, 10, 14, 17 and 26
h_F	height of the bipolar stack minus the height of terminal electrodes (cm)
I_E	current flowing through bipolar electrodes (in stack) (A)
I_s	bypass current passing through terminal electrodes and through the free space (A)
I_T	current entering the terminal electrode (A)
j	current density ($A\,cm^{-2}$)
j_o	exchange current density ($A\,cm^{-2}$)
L_E	length of the bipolar electrode (cm)
N	number of cells in stack
R_G	resistance of the electrolyte in the interelectrode gap (Ω)
R_F	resistance of the free space for $N-1$ bipolar electrodes (Ω)
R_s	resistance of the free space for one bipolar electrode (Ω)
S	surface area of the electrode (cm^2)
U	stack voltage (V)
V_r	reversible cell voltage (V)
Wa_B	Wagner number for bipolar cell, see Equation 11
w_E	width of the bipolar electrode (cm)
w_D	width of the downcomer (cm)
w_U	width of the upcomer (cm)

Greek symbols

η	overvoltage (V)
φ	Galvani potential (V)
κ_F	electrical conductivity of the electrolyte ($S\,cm^{-1}$)
κ_G	electrical conductivity in the interelectrode gap ($S\,cm^{-1}$)

Superscripts

m	in the metallic phase (electrode)
s	in the electrolyte phase at the electrode surface

Subscripts

A	anode
av	averaged
C	cathode
i	number of the electrode
k	arbitrary index
T	terminal electrode

1. Introduction

In recent years there has been an increasing interest in the use of bipolar cells for fused salt electrolysis for light metal production. The outstanding examples are the cell for the so-called 'Alcoa Smelting Process' for aluminium [1] which was tested on a pilot scale and the Alcan [2] and Ishizuka [3, 4] magnesium cells

* Permanent address: Department of Inorganic Technology, Institute of Chemical Technology, 16628 Praha 6, Czech Republic.

0021-891X

which are being used industrially. Different types of molten salt bipolar cells for electrowinning of aluminium are described in the literature [5–12].

The individual bipolar cells used in aqueous electrolytes are always connected to the main pipes via inlet and outlet manifolds made from insulating materials. These manifolds considerably reduce the magnitude of the currents bypassing the individual bipolar cells. Bypass currents (also called parasitic or shunt currents) flowing through the connecting manifolds and pipes lower the current efficiency of the bipolar cell stack. Procedures for calculation of the bypass currents and the bypass current efficiency for these systems can be found in [13–29].

In [28, 29] systems without connecting manifolds were studied. The calculation of bypass current efficiency in [28, 29] was based on the assumption, that the resistance of the ith connecting manifold (which does not exist in reality) was set equal to the resistance of the ith part of the connecting pipe (see Equation 15, p. 47 in [29]). The average bypass current efficiency was estimated experimentally [29], for the electrolysis of alkaline solution and this value agreed well with the calculated value. The agreement was due to the fact, that the space of the connecting pipe was not fully used for the flux of electric charge (see Fig. 25, page 93 [29]). Therefore the use of an additional resistance, even without good physical meaning, was necessary to obtain an agreement between calculated and measured values.

In molten salt electrochemistry outlet and inlet manifolds cannot be made to materials problems. In the Alcoa [1] and Ishikawa [11] cells for the production of liquid aluminium using aluminium chloride containing melts, a stack of bipolar electrodes are arranged in horizontal (or sloping) configuration within one cell compartment with open channels (upcomers and downcomers) to allow for circulation of the electrolyte, escape of chlorine and to collect the liquid aluminium.

A simplified description of the bypass current flow in these cells was given by Ishikawa and Konda [30]. In earlier papers [31, 32] we used the Ishikawa and Konda approach and calculated the bypass current efficiency for the pilot plant cell of the Alcoa Smelting Process.

The aim of the present paper is to test the Ishikawa and Konda procedure by using a numerical solution of the Laplace equation for the case of the Alcoa bipolar cell stack. A numerical solution should make it possible to obtain more detailed information about the influence of the bypass current flow in the free space on the current density distribution at the edges of the bipolar electrodes.

2. Description of a model system

The most advanced process using a bipolar cell stack for the production of liquid aluminium from molten chloride melts is the Alcoa Smelting Process for the electrolysis of $AlCl_3$ dissolved in an LiCl–NaCl–

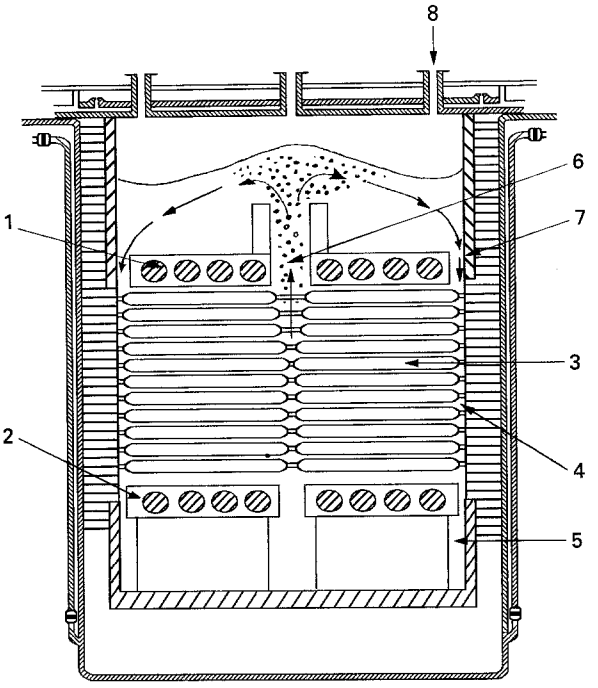

Fig. 1. Bipolar cell with horizontally placed electrodes for the Alcoa Smelting Process ($AlCl_3$ electrolysis), according to [1]. (1) Terminal anode; (2) terminal cathode; (3) bipolar electrode; (4) anode–cathode gap; (5) aluminium sump; (6) upcomer; (7) downcomer; (8) feed port.

$AlCl_3$ electrolyte using bipolar graphite electrodes [1]. In molten chloride electrolytes the anode product is chlorine, and the graphite anode is practically inert. The essential features of this cell design have been disclosed in a paper by LaCamera [1], and this cell was used in [31, 32] as an example for the calculation of the bypass current.

Figure 1 shows a cross-section of the bipolar cell stack, as described by LaCamera [1]. The bipolar electrodes consist of rectangular graphite plates placed horizontally. Slanting slots are made in the lower part (anode) of the graphite plates to facilitate the escape of the anode gas (chlorine) towards the central channel. Two rectangular bipolar electrode stacks (approx. 1.2 m wide and 5.6 m long) are placed symmetrically in one tank (approx. 2.6 m wide and 5.6 m long). At the top of the stack two dams are formed which increase the gas lift effect of the evolved chlorine bubbles and prevent back flow of electrolyte.

The direction of the electrolyte flow is denoted by arrows. The central part of the cell, where the gas–electrolyte mixture is rising, is called the upcomer (approx. 0.1 m wide and 5.6 m long) and the free space between the lining and the bipolar electrode stack form the so-called downcomers (approx. 0.05 m wide and 5.6 m long). The upcomer and the two downcomers make up the free space in the cell (filled with electrolyte or a mixture of electrolyte and chlorine gas bubbles). The aluminium is deposited on the graphite cathodes in the form of small droplets. These droplets are moved by the electrolyte flowing between the electrodes, and the major part immediately fall down in the upcomer into the aluminium sump at the bottom of the cell, while the smaller

droplets move along with the electrolyte and separate out in the downcomer.

A similar cylindrical cell with a stack of sloping bipolar graphite electrodes was proposed by Ishikawa *et al.* [11] for electrolysis of $AlCl_3$ in chloride melts. In this cell an upcomer is formed between the perimeter of the graphite electrodes and the lining of the cell, and the central part of the cell constitutes a downcomer.

3. Theory

3.1. *Flow of the bypass current according to Ishikawa and Konda*

Ishikawa and Konda [30] suggested that the total current (I_T) which enters the terminal anode and leaves the cell through the terminal cathode, can be split into the current, I_E, which flows through all bipolar electrodes in the stack, and the bypass current, I_s, which flows directly from the terminal anode to the terminal cathode in the free space filled with electrolyte or electrolyte–bubble mixture.

$$I_T = I_E + I_s \tag{1}$$

In Fig. 1 this free space is represented by the upcomer and the two downcomers. The total voltage, U, for a stack with N bipolar cells can be expressed for each cell in the stack as a sum of the reversible voltage, V_r, the voltage loss due to anodic and cathodic polarization, η_A and η_C, and the voltage loss in the interelectrode gap $R_G I_E$.

$$U = N(V_r + \eta_A - \eta_C + R_G I_E) \tag{2}$$

The average value of the resistivity of the interelectrode gap, R_G, can be calculated from the equation,

$$R_G = \left(\frac{1}{\kappa_G}\right)\frac{d_{G,av}}{A_E} \tag{3}$$

where the average interelectrode gap, $d_{G,av}$, is given by a fictitious cell through which the bypass current I_s flows in the free space with a fictitious anode plate located in the free

$$d_{G,av} = \frac{\Sigma d_{G,i}}{N} \tag{4}$$

space at the position of the terminal anode and with a fictitious cathode plate located in the free space at the position of the terminal cathode. The total voltage of this cell is also equal to U. The voltage balance valid for this cell is given by the equation,

$$U = V_r + \eta_A - \eta_C + R_F I_s \tag{5}$$

To simplify the calculation, the values for the overvoltages for the fictitious cell is assumed to be equal to the overvoltages used for the bipolar cell. The resistance R_F in the free space of the fictitious cell can be expressed as

$$R_F = \left(\frac{1}{\kappa_F}\right)\frac{h_F}{A_F} \tag{6}$$

where the height of the upcomer (or downcomer), h_F, is set equal to the height of the cell stack minus the height of the terminal electrodes

$$h_F = Nd_G + (N-1)d_E \tag{7}$$

and A_F is the cross-sectional area of all upcomers and downcomers. The cell stack with N cells contains $N-1$ bipolar electrodes and altogether $N+1$ electrodes including the terminal electrodes.

Equation 6 is valid for a fictitious cell located in the free space with an interelectrode distance, h_F, and the cross-sectional area, A_F, through which the bypass current flows. For the stack shown in Figs 1 and 2, A_F is represented by the averaged cross-sectional area of the downcomers and the upcomer (the area is determined in the direction normal to the current flow). A reasonable value for f_E can be found by using the specific conductivity of the electrolyte, κ_F, neglecting the presence of bubbles in the upcomer of the free space. In the interelectrode gap the gas partly travels in the slots made in the anode, but the decrease in electrolyte conductivity, κ_G, may still be significant. By the use of Equations 1, 2 and 5 I_s can be evaluated

$$I_s = \frac{(N-1)(V_r + \eta_A - \eta_C) + NR_G I_T}{R_F + NR_G} \tag{8}$$

According to Ishikawa [30] 'the bypass current efficiency' or 'the utilization of the current for the electrochemical process' for bipolar cells used in molten salt electrolysis (f_E) is given by the equation

$$f_E = \frac{I_T + (N-1)I_E}{NI_T} \tag{9}$$

with the use of Equations 1, 8 and 9 the bypass current efficiency may be expressed as

$$f_E = 1 - \frac{(N-1)[(N-1)(V_r + \eta_A - \eta_C) + NR_G I_T]}{N(R_F + NR_G)I_T} \tag{10}$$

Equations 1–10 represent a simple approximation for the bypass current flow and for the bypass current efficiency f_E for a given cell geometry and a given electrochemical cell reaction.

According to [29] a Wagner number for a bipolar cell can be introduced as

$$Wa_B = \frac{(V_r + \eta_A - \eta_C)}{j_T}\frac{\kappa_G}{d_{G,av}} \tag{11}$$

Futhermore two dimensionless parameters can be introduced:

$$a = \frac{w_E}{(w_U + w_D)}\frac{\kappa_G}{\kappa_F} \tag{12}$$

$$b = \frac{d_E}{d_{G,av}} \tag{13}$$

By means of Equations 11, 12 and 13 Equation 10 can be rewritten into the dimensionless form,

$$f_E = 1 - \frac{Wa_B + 1}{a + ab + 1} + \frac{N[Wa_B(2a + ab + 2) + a + 1] - Wa_B(a + ab + 1)}{N^2(a + ab + 1)^2 - Nab(a + ab + 1)} \tag{14}$$

The second term on the right hand side of Equation 14 is prevailing over the third term. For N greater than 10 the third term represents approximately 10% of the second term. This means, that the second term is the most important one and can be used for an analysis of a given system.

3.2. *Flow of the bypass current according to [14]*

According to [14] the terminal plates and one half of the interelectrode gaps adjacent to the terminal electrodes form a fictitious cell, through which the current I_T flows. Each bipolar electrode with one half of the interelectrode gap on both sides represents another fictitious cell, which is short-circuited by a resistor R_s

$$R_s = \frac{1}{\kappa_F} \frac{(d_{G,av} + d_E)}{A_F} \tag{15}$$

The voltage balance for each bipolar electrode then reads:

$$V_r + \eta_A - \eta_C + R_G I_E = R_s I_s \qquad i = 2, 3, \ldots, N \tag{16}$$

Using Equations 1, 9, 11, 12 and 13 the bypass current efficiency can be evaluated as

$$f_E = 1 - \frac{Wa_B + 1}{a + ab + 1} + \frac{Wa_B + 1}{N(a + ab + 1)} \tag{17}$$

For large values of N the limiting values of f_E calculated from Equations 14 and 17 are identical. The differences between f_E values calculated from Equations 14 and 17 for N greater than 10 are lower than 0.4% for the present case. The f_E values calculated from Equation 17 are higher than the values calculated from Equation 14 for d_E greater than 8 cm for the studied case, see Fig. 3.

3.3. *Solution of the Laplace equation for a stack of bipolar electrodes*

A more accurate value for the bypass current and for the bypass current efficiency f_E can be obtained by solving the Laplace equation for the space filled with electrolyte, e.g. for all of the interelectrode gaps and for the free volume. Because the conductivity varies in the mentioned space, the Laplace equation has the form,

$$\nabla \cdot (\kappa \nabla \varphi) = 0 \tag{18}$$

where φ is a Galvani potential in the electrolyte.

3.4. *Boundary conditions*

For the estimation of the Galvani potentials in the graphite bipolar electrodes it is necessary to fulfil the following integral boundary condition, for each of the i bipolar electrodes*;

$$\oint j \, dS_i = 0 \qquad i = 2, 3, \ldots, N \tag{19}$$

In Equation 19 S_i represents the surface of the ith bipolar electrode and j_n represents local current density. Fulfilling the conditions given by Equation 19, the values of the Galvani potential in each of the i graphite bipolar electrodes are determined. The Galvani potentials in each electrode are considered as constants, the Laplace equations for the electrode material of each of the $(N-1)$ bipolar electrodes are not solved, i.e. the voltage drop in the electrode material is neglected. The electrical conductivity of graphite is more than two orders of magnitude higher than that of the electrolyte, so this simplification should be justified.

The anodic and cathodic potentials as functions of the current density for both electrodes should be known, because they serve as boundary conditions located on the surface of all bipolar and terminal graphite electrodes. For the anodic reaction

$$Cl^- = \tfrac{1}{2} Cl_2 + e^- \tag{20}$$

a Butler–Volmer equation was used. The charge transfer coefficients are assumed to be equal to 0.5 for both electrode reactions.

$$j = j_o[\exp(\eta/b) - \exp(-\eta/b)] \tag{21}$$

The anodic potential is equal to the sum of the reversible anodic potential $E_{r,A}$ and the anodic overvoltage η_A

$$E_A = E_{r,A} + \eta_A \tag{22}$$

For the cathodic reaction it is known [33] that $AlCl_3$ forms $AlCl_4^-$ complexes, hence

$$AlCl_4^- + 3e^- = Al + 4Cl^- \tag{23}$$

Also in this case it is assumed that the relationship between the current density and the overvoltage is represented by Equation 21 for low current densities or by a Tafel type of plot for high current densities. The cathodic polarization is relatively low [33]. It is dominated by concentration overvoltage [33], but polarization curves measured for the deposition of aluminium from chloride melts on graphite electrodes were not found in the literature. However, it is known from other systems that even in such cases a Tafel type of behaviour may be observed [34]. The cathodic potential is equal to the sum of the reversible cathodic potential $E_{r,C}$ and the cathodic overvoltage η_C,

$$E_C = E_{r,C} + \eta_C \tag{24}$$

The electrode potentials are defined as the difference between the Galvani potential in the metal φ^m and

* The following numbering of electrodes was adopted: the top terminal electrode (anode) was electrode number one, the first bipolar electrode located below the terminal anode was number two, the last bipolar electrode in the cell stack (above the terminal cathode) was electrode number N and the bottom terminal electrode (cathode) was number $(N+1)$.

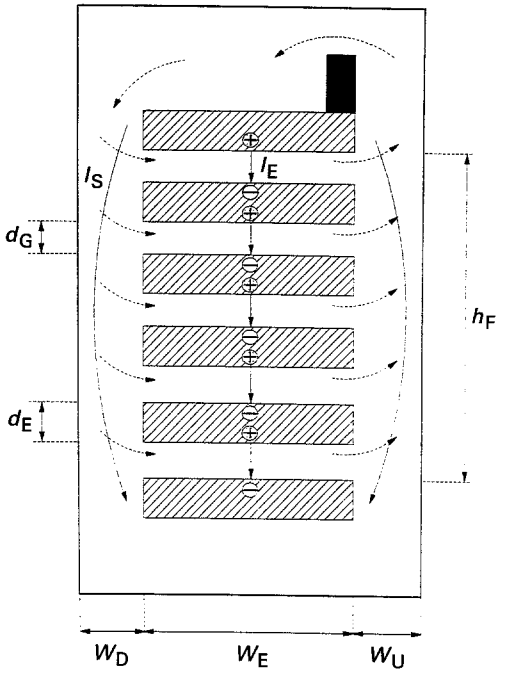

Fig. 2. Sketch of the current flow and the geometry for a bipolar electrode stack with horizontal electrodes. I_E, I_S, w_D, w_U, w_E, h_F, d_G, d_E defined in text. Dashed arrows: electrolyte flow; full arrows: current flow.

in the solution of φ^s at the electrode surface.

$$E_k = \varphi_k^m - \varphi_k^s \qquad k = A, C \tag{25}$$

It should be mentioned that for all electrode potentials of a bipolar electrode, which are located between the reversible voltage of the cathode and the reversible voltage of the anode, the current density was set equal to zero. These electrode potentials are present on the side walls of the bipolar electrodes. The real situation for this special range of the electrode potentials will be different, and it may be assumed that two different reactions, one anodic and one cathodic, proceed simultaneously. Low current densities, either anodic or cathodic, can be expected in this range of electrode potentials. This means that an ill-defined mixed electrode potential is established for the 'near zero' current density. An estimation of the polarization curves for this range of electrode potentials was not possible. However, in the total current balance for each bipolar electrode, the side surface of a bipolar electrode represents only a few percent of the total electrode surface area, so even large errors made in this region are unimportant.

4. Discussion

4.1. *Loss in current efficiency due to bypass current*

The solution of the Laplace Equation 10 was performed using the method of finite differences. A method of adding the current densities over the surface of the control volume was used, e.g. a conservative scheme was used. This method gives exact values of fluxes even for varying electrical conductivity in the space. The method is described in detail in [35].

The so-called secondary current distribution for all bipolar electrodes and terminal electrodes in the stack was calculated using boundary conditions represented by Equation 13. The integral of the current densities over the surface of the terminal anode and terminal cathode is equal to the total current I_T, and the integral of the anodic or cathodic current densities for one side of the bipolar electrode (and appropriate part of the side wall of the electrode) represents the value of the current $I_{E,i}$ flowing through the ith bipolar electrode. These currents ($I_{E,i}$) vary with the position of the ith bipolar electrode in the stack. The currents $I_{E,i}$ are not symmetrical compared to the central bipolar electrode, e.g. $I_{E,2}$ is not equal to $I_{E,N}$ etc., due to different polarization curves used for the anodic and cathodic reactions.

The f_E value was calculated from the equation

$$f_E = \frac{I_T + \Sigma I_{E,i}}{N I_T} \tag{26}$$

The calculation of the bypass current efficiency (f_E) was performed using the geometry and dimensions of the Alcoa bipolar cell stack given in [1]. An important parameter for the bipolar cell stack is the thickness of the bipolar graphite electrodes, since it determines the height of the stack, once the interelectrode distance is given. For the Alcoa cell this thickness is $d_E = 10.8$ cm [36]. According to [1], the bipolar graphite electrodes had sloping slots for the chlorine gas collection (on the underside of the bipolar electrodes). The solution for the Laplace equation was performed for plate electrodes in two dimensional space. The presence of the slots was accounted for in the value of the effective electrical conductivity, κ_G, used for the gas–electrolyte mixture in the interelectrode gap.

The Laplace Equation 10 was solved using the following input data: the total current I_T flowing through the cell, 120 000 A, the surface floor, 14.4 m^2 (2.56 m wide and 5.64 m long), the bipolar electrode area, 12 m × 13.5 m (two stacks, each 1.2 m wide, w_E, and 5.64 m long, L_E), the interelectrode distance, d_G 1.27 cm (above the terminal cathode 1.91 cm). The total area, A_F, of the two downcomers $2w_D L_E$ and the upcomer $2w_U L_E$, was set equal to 0.97 m^2, the width of the downcomer, w_D 4.3 cm and the width of one half of the upcomer 4.3 cm, w_U. The electrical conductivity was estimated to be $\kappa_F = 3.58$ S cm^{-1} [33] for the composition of the melt used by Alcoa at a temperature of 1000 K. This value of conductivity agrees with conductivity data given by Kinosz and Haupin [37]. The electrical conductivity in the interelectrode gap, κ_G, was estimated to be 2.58 S cm^{-1} based on assumptions concerning gas filling and the presence of slots in the anodes for collecting the anode gas [36]. The anodic overvoltage for 0.89 A cm^{-2} was assumed to be 0.20 V, based on unpublished data by Ytterdal [38], the cathodic overvoltage was assumed to be −0.1 V, based on analogy with similar systems [34]. The reversible voltage was taken to be 2.05 V [39]. The values of the Tafel slopes

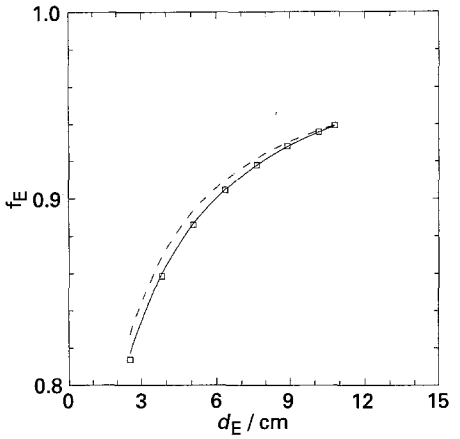

Fig. 3. Current efficiency, f_E, based on the bypass current against the thickness of the bipolar electrode d_E calculated for the case of the Alcoa cell for $AlCl_3$ electrolysis (see text) using Equation 14 (full line); numerical solution of the Laplace equation in the inter-electrode and free space: (dashed line); (□) Equation 17.

of the polarization curves (see Equation 13), b_A, b_C were assumed to be 0.086 V and 0.057 V, respectively. The values of anodic and cathodic exchange current densities were assumed to be 0.088 A cm^{-2} and 0.16 A cm^{-2}, respectively. The calculation was carried out for a stack of 12 bipolar cells ($N = 12$). The dimensionless parameters for the studied case were $Wa_B = 5.17$, $a = 10.06$ and $b = 8.16$.

The calculated total voltage for the stack, U, was 33.3 V for $d_B = 10.8$ cm. This value is reasonably close to the value derived from data given by LaCamera [1] being 31.2 V, which is probably the minimum value.

Figure 3 shows a plot of f_E against the thickness of the bipolar plate. Calculations made for different values of the thickness of the bipolar electrodes, showed that this thickness can change the value of f_E considerably, because at the same time the height of the cell and the height of the free volume are changed. Values of f_E calculated by means of the theory of Ishikawa and Konda are also given in Fig. 3. The values calculated by using Equation 17 fall in all cases between the values calculated numerically and the values calculated from Equation 14. It means, that Equation 17 represents better approximation than Equation 14.

4.2. *Current distribution*

The average values of current densities for each bipolar electrode are shown in Fig. 4. The values of $I_{E,i}$ in Fig. 4 are very close to each other for different values of i, the greatest difference between the average current densities is always between the terminal and the first (or last) bipolar electrode.

The values of $I_{E,2}$ are not equal to the values of $I_{E,N}$, e.g. a symmetry with respect to the central electrode does not exist. There are two reasons for the asymmetry in the values of $I_{E,i}$. The asymmetry is partly due to the different polarization curves used for the anodic and cathodic processes and partly due to the different heights of the interelectrode gaps

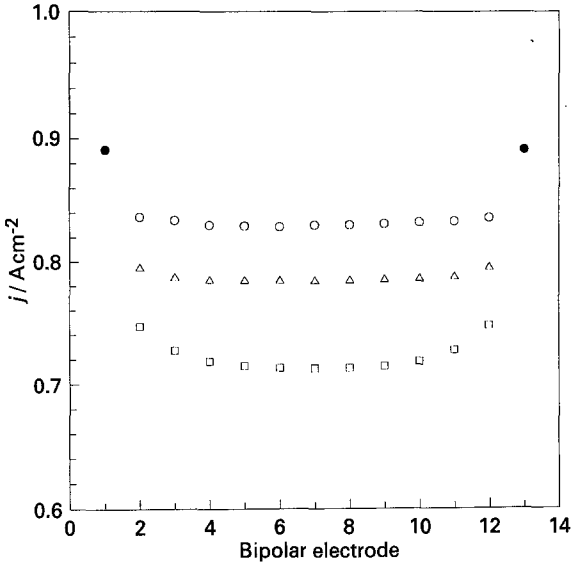

Fig. 4. Dependence of the average current density for the ith electrode on the position of ith bipolar electrode in the cell stack. Average current density for terminal electrodes: (○) for $d_E = 10.8$ cm, $h_F = 134.6$ cm; (△) for $d_E = 5.08$ cm, $h_F = 71.8$ cm; (□) for $d_E = 2.54$ cm, $h_F = 43.8$ cm.

(the height of the gap at the terminal cathode was 1.91 cm, while the heights of all other gaps were 1.27 cm [1]).

Figure 5 shows the current density distribution along the terminal anode. The origin of the coordinates is placed in the left bottom corner of the terminal anode. The x direction is along the inter-electrode gap, the y direction is oriented normal to it. As expected, the highest current densities are at the edges of the terminal electrode ($x = 0, y = 0$), which also cause a considerable decrease in current densities around the edge of the cathodic side of the first bipolar electrode, as shown in the following.

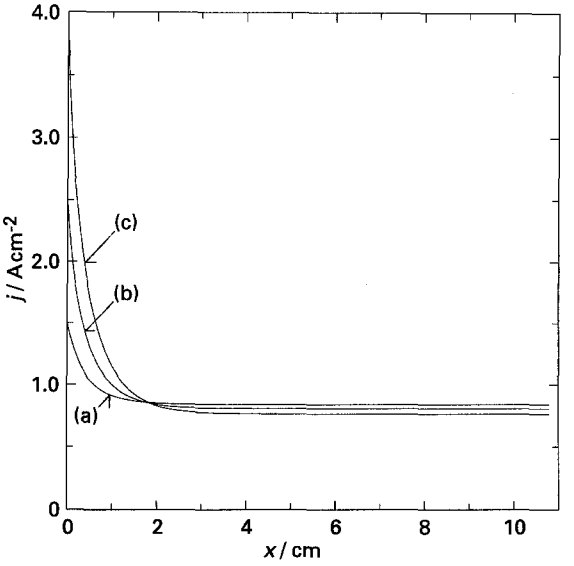

Fig. 5. Dependence of the anodic local current density for the terminal electrode (electrode 1) on the distance from the left bottom edge ($x = 0, y = 0$) in the x direction (in the interelectrode gap). Average current density for the terminal electrode 0.89 A cm^{-2}. (a) for $d_E = 10.8$ cm, $h_F = 134.6$ cm, (b) for $d_E = 5.08$ cm, $h_F = 71.8$ cm, (c) for $d_E = 2.54$ cm, $h_F = 43.8$ cm.

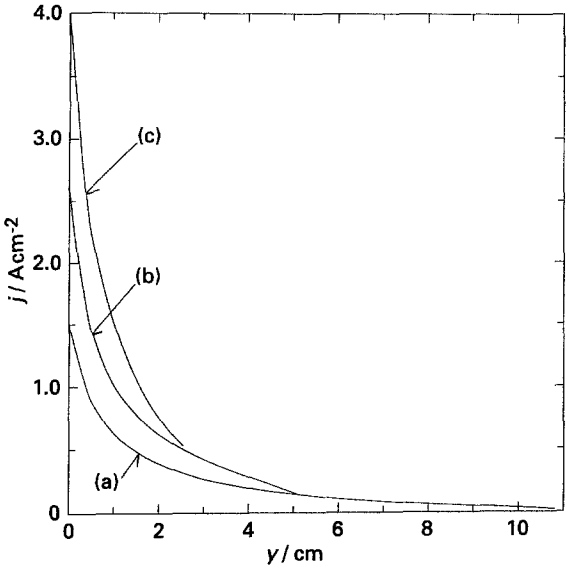

Fig. 6. Dependence of the anodic local current density for the terminal electrode (electrode 1) on the side wall of the anode on the distance from the left bottom edge ($x = 0, y = 0$) in the y direction. For average current density and the notation of the curves, see Fig. 5.

The local current densities along the side wall of the terminal anode (in the y direction) are shown on Fig. 6. These local values of c.d. depend considerably on the values of d_E or h_F. Current densities for the upper surface of the terminal anode are given in Fig. 7 in the x direction. It was assumed that the height of the melt above the terminal anode is 20 cm, so the upper surface of the terminal electrode was quite well accessible for anodic current in the case of a thin graphite electrode.

The strong influence of the current flowing out from the interelectrode gap from the terminal anode plate into the free space leading to a decrease of the local current densities at the upper left edge of the first bipolar electrode (cathode) can be seen in Fig. 8.

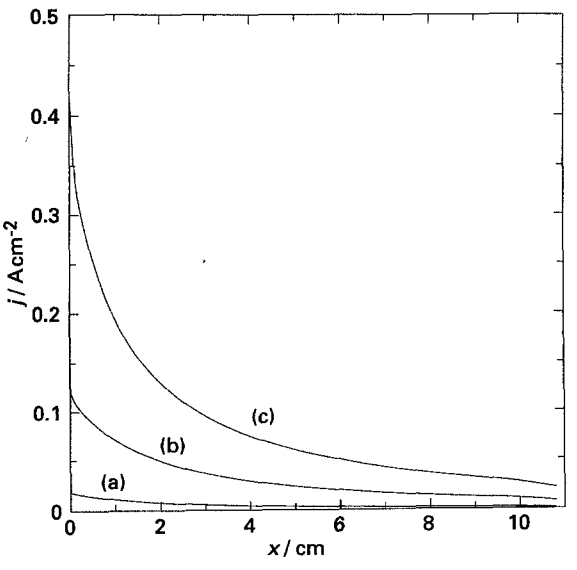

Fig. 7. Dependence of the anodic local current density for the terminal electrode (electrode 1) on the upper surface of the anode on the distance from the left top edge. The origin of the coordinates is shifted to the point ($x = 0, y = d_E$). For average current density and the notation of the curves, see Fig. 5.

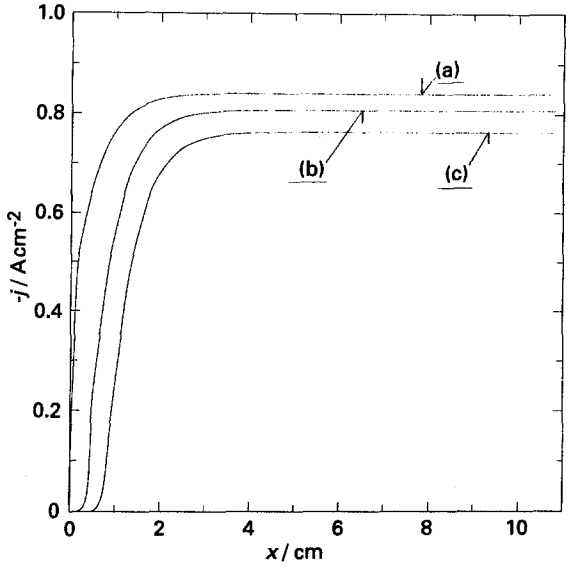

Fig. 8. Dependence of the cathodic local current density for the first bipolar electrode (electrode 2) on the distance from the left top edge in the x direction (in the interelectrode gap). The origin of the coordinates is shifted to the point ($x = 0, y = -d_G$). For average current density and the notation of the curves, see Fig. 5.

The decrease of the local current densities at the upper left edge of the first bipolar electrode depends considerably on the thickness of the bipolar electrodes. This effect may be the reason why the introduction of a fictitious cell with height h_F was so successful in the calculation of the bypass current efficiency, using Equation 14. The very good agreement between such a simple description of a very complicated system and the exact solution of the Laplace equation for Galvani potentials in the cell stack, shown in Fig. 3, could not be anticipated *a priori*.

The anodic current densities for a bottom surface of the first bipolar electrode (electrode 2) are shown on Fig. 9. The shape of these curves is similar to that of the anodic c.d. for the terminal electrode, see Fig. 5.

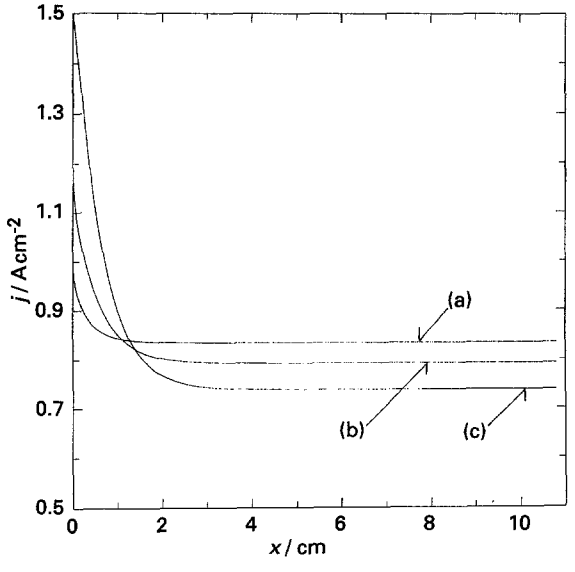

Fig. 9. Dependence of the anodic local current density for the first bipolar electrode (electrode 2) on the distance from the left bottom edge in the x direction (in the interelectrode gap). The origin of the coordinates is shifted to the point ($x = 0, y = -d_G - d_E$). For average current density and the notation of the curves, see Fig. 5.

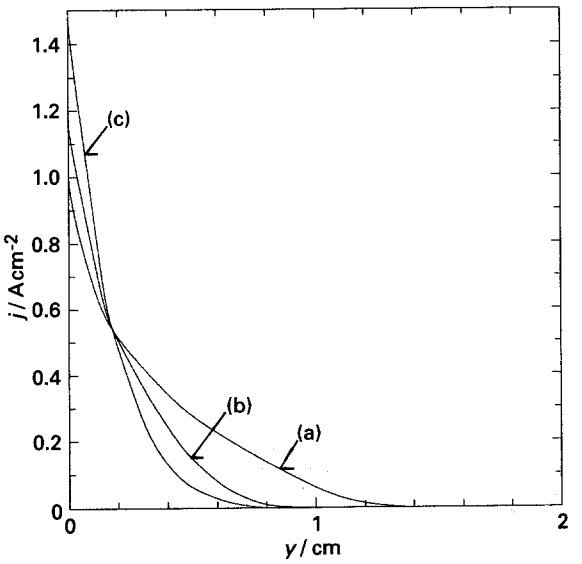

Fig. 10. Dependence of the anodic local current density for the first bipolar electrode (electrode 2) on the side wall of the anode on the distance from the left bottom edge in the y direction. The origin of the coordinates is shifted to the point $(x = 0, y = -d_G - d_E)$. For average current density and the notation of the curves, see Fig. 5.

Figure 10 shows anodic c.d.'s on the sidewall of electrode 2. The c.d. shows high values near the edge of the anodic side of electrode 2. For the cathodic side of the second bipolar electrode, see Fig. 11, a new shape of the c.d. is present for $d_E = 10.8$ cm. The local c.d. is very close to the average value of the c.d. on the given electrode surface, with only a small rise near the edge of the electrode. This type of c.d. distribution is then present at all the other bipolar electrodes with the exception of the last one. High values of c.d. are also present near the edge on the side walls of the bipolar electrodes. These small effects are caused by the outer electric field due to the passage of the bypass current through the downcomer which interferes with the electric field due to the passage of the current through the bipolar electrodes.

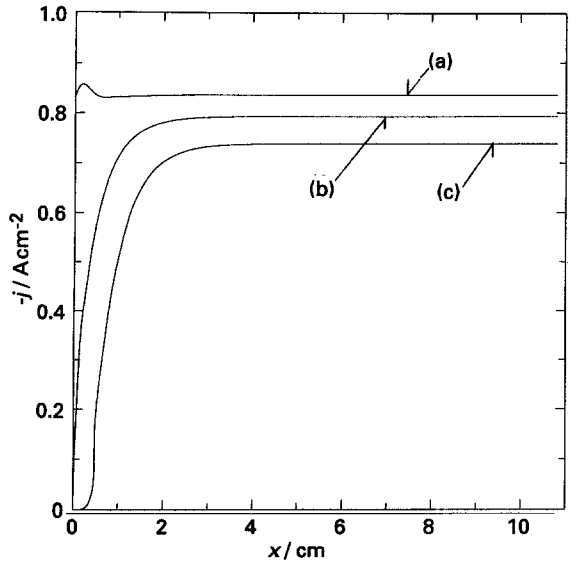

Fig. 11. Dependence of the cathodic local current density for the second bipolar electrode (electrode 3) on the distance from the left top edge in the x direction (in the interelectrode gap). The origin of the coordinates is shifted to the point $(x = 0, y = -2d_G - d_E)$. For average current density and the notation of the curves, see Fig. 5.

Curves 2 and 3 on Fig. 11 indicate that, in those cases some bypass current is still flowing out from the second anodic plate into the downcomer. However this effect is considerably smaller than for the first cell created by the terminal anode and the cathode of the first bipolar electrode.

The shapes of the curves on Figs 5, 6, 7 and 8 are repeated for the opposite electrodes at the end of the bipolar stack.

It was assumed, that the bottom surface of the terminal cathode is also accessible for the current. The difference between the level of the liquid aluminium in the sump and the bottom surface of the cathode was assumed to be 20 cm, but this distance varies with time.

Figures 4–11 show the effect of different thicknesses of the bipolar electrodes and/or of different heights of the free space. The decrease of the local current densities near the edge for the first and last bipolar electrodes (cathodic and anodic side, respectively) and the shift of this decrease along the electrode towards the central part of the stack when lowering the height of the bipolar stack, explain the decrease of the bypass current efficiency with decreasing height, as seen in Fig. 3.

5. Summary

The possibility of the use of the simple Ishikawa and Konda approach [30] or the approach according to [14] with the introduction of fictitious cells, in both cases, was confirmed by solution of the Laplace equation for the Alcoa pilot plant bipolar cell stack. The differences in the calculated bypass current efficiencies, using both methods, were less than 1.3% for all cases, when the thickness of bipolar plates was greater than 2.54 cm.

Acknowledgement

This work was supported by the Royal Norwegian Council for Scientific and Industrial Research (NTNF) by a Senior Scientist Fellowship to one of the authors (I.R.) and by NTH, Trondheim, Department of Electrochemistry for computing facilities. Information on the Alcoa Smelting Process given by Alfred LaCamera of Alcoa and by Warren Haupin (Formerly Alcoa) is gratefully acknowledged.

References

[1] A. F. LaCamera, Mathematical Modelling of Materials Processing Operations, TMS – AIME Extractive and Process Metallurgy Fall Meeting, Palm Desert, CA, Oct. 2–Nov. 29 (1987) pp. 671–691.

[2] O. G. Sivilotti and A. Briand, *US Patent 3 396 094*, 6 Aug. (1968). O. G. Sivilotti, *US Patent 4 055 474*, 25 Oct. (1977). *US Patent 4 518 475*, 21 May (1985). *US Patent 4 514 269*, 30 Apr. (1985). *US Patent 4 560 449*, 24 Dec. (1985).

[3] H. Ishizuka, *US Patent 4 495 037*, 24 Jan. (1985). *US Patent 4 647 355*, 3 Mar. (1987).
[4] N. Høy-Pettersen, T. Aune, T. Vralstad, K. Andreassen, D. Øymo, T. Haugerød and O. Skaane, 'Magnesium', in Ullmann's 'Encyclopedia of Industrial Chemistry', Vol. A15 VCH Publ. (Weinheim, 1990) pp. 559–580.
[5] G. de Varda, *US Patent 3 554 893*, 12 Jan. (1971).
[6] N. Feng, Z. Qui, K. Grjotheim and H. Kvande, 'Light Metals 1990', TMS – AIME, Warrendale, PA (1990) pp. 379–383.
[7] H. Alder, *US Patent 3 930 967*, 6 Jan. (1976).
[8] *German Patent 2 805 374.9*, 9 Feb. (1978), Vereinigte Aluminiumwerke.
[9] D. Darracq, J. J. Duruz and C. Durmelat, *Internat. Pat. Appl. WO 88/01313*, 25 Feb. (1988).
[10] E. H. Rogers, S. C. Jacobs, L. L. Knapp and W. R. Allen, *US Patent 4 140 594*, 20 Feb. (1979). *US Patent 4 133 727*, 9 Jan. (1979).
[11] T. Ishikawa, S. Konda, T. Iuchi and H. Ichikawa, *US Patent 4 151 061*, 15 Nov. (1979).
[12] Y. Bertaud, *US Patent 4 459 195*, 10 July (1984).
[13] R. Wilson, 'Demineralization by Electrodialysis', Butterworth's, London (1960) p. 265.
[14] I. Rousar, *J. Electrochem. Soc.* **116** (1969) 676.
[15] I. Rousar and V. Cezner, *ibid.* **121** (1974) 648.
[16] M. Katz, *ibid.* **125** (1974) 515.
[17] O. S. Ksenzhek and N. D. Koshel, *Elektrokhimiya* **7** (1971) 353.
[18] V. A. Onishchuk, *ibid.* **8** (1972) 689.
[19] B. P. Nesterov, G. A. Kamzelev, V. F. Gerasimenko and N. V. Korovin, *ibid.* **9** (1973) 1154.
[20] E. A. Kaminski and R. P. Savinell, *J. Electrochem. Soc.* **130** (1983) 1103.
[21] J. C. Burnett and D. E. Danly, *AIChE Symposium Series No. 185* **75** (1979) 8.
[22] W. Thiele, M. Schleiff and H. Matschiner, *Electrochim. Acta* **26** (1981) 1005.
[23] J. W. Holmes and R. E. White, in 'Electrochemical Cell Design' (edited by R. E. White), Plenum, New York (1984) p. 331.
[24] R. E. White, C. W. Walton, H. S. Burney and R. N. Beaver, *J. Electrochem. Soc.* **133** (1986) 485.
[25] R. E. White, H. S. Burney and R. N. Beaver, in 'Modern Chlor-Alkali Technology', Vol. 3 (edited by K. Wall), Ellis Horwood, Chichester, UK (1986) p. 365.
[26] G. Zhao, S. Duan, Q. Tian and T. Wu, *Metall. Trans. B* **21B** (1990) 783.
[27] Min-Zhi Yang, H. Wu, R. Selman, *J. Appl. Electrochem.* **19** (1989) 247.
[28] P. Bolomey, PhD thesis no. 753, EPFL, Lausanne (1988).
[29] G. Bonvin, PhD thesis no. 1029, EPFL, Lausanne (1992).
[30] T. Ishikawa and S. Konda, Proceedings of the 1st International Symposium on Molten Salt Chemical Technology, Kyoto, 20–22 Apr. (1983) p. 5.
[31] T. R. Beck, I. Rousar and J. Thonstad, 'Light Metals 1993', TMS – AIME, Warrendale, PA (1993) pp. 485–491.
[32] T. R. Beck, I. Rousar, J. Thonstad, *Trans. Metall. B*, to be published.
[33] R. Ødegard, A. Bjørgum, Å. Sterten, J. Thonstad and R. Tunold, *Electrochim. Acta* **27** (1982) 1595.
[34] J. Thonstad and S. Rolseth, *ibid.* **23** (1978) 223.
[35] I. Rousar, K. Micka and A. Kimla, 'Electrochemical Engineering', Vol. 1, Elsevier, Amsterdam, and Academia, Praha (1986) p. 136.
[36] A. F. LaCamera, private communication with authors, Alcoa Technical Center, Alcoa Center, PA 15069.
[37] D. L. Kinosz and W. Haupin, Proceedings of the International Symposium on Molten Salts, Washington DC, Electrochemical Society, Princeton, NJ (1976) pp. 375–382.
[38] S. Ytterdal, MSc thesis, NTH, Trondheim (1975).
[39] A. Björgum, Å. Sterten, J. Thonstad and R. Tunold, *Electrochim. Acta* **26** (1981) 487, 491.